

Targeting the Spleen Tyrosine Kinase with Fostamatinib as a Strategy Against Waldenström's Macroglobulinemia

Isera Kuiatse¹, Veerabhadran Baladandayuthapani², Heather Y. Lin², Sheeba K. Thomas¹, Chad C. Bjorklund¹, Donna M. Weber¹, Michael Wang¹, Jatin J. Shah¹, Xing-Ding Zhang¹, Richard J. Jones¹, Stephen M. Ansell³, Guang Yang⁴, Steven P. Treon⁴, and Robert Z. Orlowski^{1,5,*}

The Department of ¹Lymphoma/Myeloma, Department of ²Biostatistics, and Department of ⁵Experimental Therapeutics, The University of Texas MD Anderson Cancer Center, Houston, TX;

The ³Division of Hematology, Mayo Clinic, Rochester, MN; and
The ⁴Dana Farber Cancer Institute, Harvard Medical School, Boston, MA.

Address Correspondence to:

Dr. Robert Z. Orlowski, The University of Texas MD Anderson Cancer Center, Department of Lymphoma & Myeloma, 1515 Holcombe Blvd., Unit 429, Houston, TX 77030-4009, E-mail: rorlowsk@mdanderson.org, Telephone 713-794-3234, Fax 713-563-5067

Conflict of Interest Statement:

The authors have no relevant conflicts of interest to disclose with respect to this submission.

Statement of Translational Relevance

Novel therapies are needed for Waldenström's macroglobulinemia, since the currently available standard and novel agents induce high overall response rates but few patients achieve complete remission, and none are cured of this lymphoproliferative disorder. The current study validates use of the Spleen tyrosine kinase inhibitor fostamatinib as an attractive strategy using cell lines and primary samples *in vitro*, as well as a xenograft model *in vivo*. Since fostamatinib is currently undergoing clinical testing, our data provide a rationale for translation of this drug into trials targeting patients with relapsed and/or refractory, and possibly even newly diagnosed Waldenström's macroglobulinemia.

Abstract

Purpose: Waldenström's macroglobulinemia (WM) is a lymphoproliferative disorder characterized by good initial responses to standard therapeutics, but only a minority of patients achieve complete remissions, and most inevitably relapse, indicating a need for novel agents. B-cell receptor signaling has been linked to clonal evolution in WM, and Spleen tyrosine kinase (Syk) is over-expressed in primary cells, suggesting that it could be a novel and rational target.

Experimental Design: We studied the impact of the Syk inhibitor fostamatinib on BCWM.1 and MWCL-1 Waldenström's-derived cell lines both *in vitro* and *in vivo*, as well as on primary patient cells.

Results: In WM-derived cell lines, fostamatinib induced a time- and dose-dependent reduction in viability, associated with activation of apoptosis. At the molecular level, fostamatinib reduced activation of Syk and Bruton's tyrosine kinase, and also downstream signaling through mitogen activated protein kinase (MAPK) kinase (MEK), p44/42 MAPK, and protein kinase B/Akt. As a single agent, fostamatinib induced tumor growth delay in an *in vivo* model of WM, and reduced viability of primary WM cells, along with inhibition of p44/42 MAPK signaling. Finally, fostamatinib in combination with other agents, including dexamethasone, bortezomib, and rituximab, showed enhanced activity.

Conclusions: Taken together, these data support the translation of approaches targeting Syk with fostamatinib to the clinic for patients with relapsed, and possibly even newly diagnosed Waldenström's.

Introduction

Signaling through the B-cell receptor (BCR) occurring through both antigen-dependent and -independent mechanisms appears to play an important role in the pathobiology of several common B-cell malignancies. BCR aggregation results in phosphorylation of the Ig α (CD79a) and Ig β (CD79b) immunoreceptor tyrosine-based activation motifs (ITAMs), catalyzed by members of the Src family of kinases (SFKs), such as Lyn. Phosphorylated ITAM residues then serve as docking sites for the spleen tyrosine kinase (Syk), and binding results in a conformational change that facilitates exposure of tyrosines 348 and 352 for phosphorylation by SFKs, as well as Syk auto-phosphorylation. Later association with other signaling intermediates, such as Shc, Bruton's tyrosine kinase (BTK), phospholipase C gamma 2, and phosphoinositide 3-kinase, results in downstream activation of signal transduction pathways crucial to lymphoma pathobiology. Among these are the proliferation-associated mitogen-activated protein kinases (MAPKs) such as p44/42, and the survival-associated protein kinase B/Akt (1, 2).

Waldenström's macroglobulinemia is diagnosed in the presence of a lymphoplasmacytic B-cell lymphoma involving the bone marrow and a serum immunoglobulin M (IgM) monoclonal protein (3). Though this disease typically has an indolent clinical course, its presenting features can include symptomatic anemia, thrombocytopenia, hepatosplenomegaly, and lymphadenopathy, among others, and currently available therapies are not curative. At the molecular level, recent studies have identified the L265P mutation of Myeloid differentiation primary response gene 88 (MYD88) as a commonly recurring abnormality in Waldenström's patients (4-8). This mutation contributes to disease pathobiology through activation of nuclear factor kappa B signaling (4), as well as of BTK (9), implicating a role for BCR signaling. Indeed, previous studies had linked B-cell receptor signaling to clonal evolution in Waldenström's (10). These findings led to translation of the BTK inhibitor ibrutinib (11) to the clinic for patients with relapsed and/or

refractory Waldenström's. In this setting, ibrutinib showed significant anti-tumor activity (12), with a response rate of 81%, though no complete remissions were noted.

With this validation of BCR signaling as a target in Waldenström's, we considered the possibility that other intermediates could be attractive as well. We focused in particular on Syk given the availability of fostamatinib, a specific and clinically relevant (13) Syk inhibitor, and previous findings showing that Syk was over-expressed in primary patient cells (14). In the current report, we present data showing the activity of fostamatinib against pre-clinical models of Waldenström's both *in vitro* and *in vivo*, and dissect some of its mechanisms of action.

Materials and Methods

Reagents. Fostamatinib disodium (FosD; R935788) and bortezomib were purchased from Selleck Chemical (Houston, TX), and stock solutions were prepared in phosphate-buffered saline (PBS) and dimethyl-sulfoxide (Fisher Scientific; Pittsburg, PA), respectively. Rituximab was purchased from the MD Anderson Pharmacy, while dexamethasone was from Sigma-Aldrich (St. Louis, MO), with stock solutions made in PBS and ethanol (Fisher Scientific), respectively.

Tissue culture and patient samples. The BCWM.1 cell line derived from a patient with Waldenström's (15) was from Dr. Steven Treon (Dana Farber Cancer Institute; Boston, MA). These cells are CD5⁻, CD10⁻, CD19⁺, CD20⁺, CD23⁺, CD27⁻, CD38⁺, CD138⁺, CD40⁺, CD52⁺, CD70⁺, CD117⁺, clgM⁺, clgG⁻, clgA⁻, ckappa⁻, and clambda⁺ (15), and harbor the MYD88 L265P mutation but have a wild-type C-X-C chemokine receptor type 4 (CXCR4)(16). MWCL-1 Waldenström cells were from Dr. Stephen Ansell (The Mayo Clinic; Rochester, MN)(17), and are CD3⁻, CD19⁺, CD20⁺, CD27⁺, CD38⁺, CD49D⁺, CD138⁺, clgM⁺, and kappa⁺. They also harbor the MYD88 L265P mutation and a wild-type CXCR4(16), but have a TP53 missense mutation at exon 5 (V143A, GTG>GCG)(17). BWCM-1 cells were propagated in RPMI 1640 media (Life Technologies; Grand Island, NY) supplemented with 2 mM L-glutamine (Invitrogen; Carlsbad, CA) and 10% fetal calf serum (Hyclone; Logan, UT), while MWCL-1 cells were grown in similarly supplemented IMDM (Life Technologies). All cultures also contained 100 U/mL penicillin and 100 µg/mL streptomycin (Mediatech; Manassas, VA). Cell line authentication was performed by the MD Anderson Characterized Cell Line Core Facility using short tandem repeat DNA fingerprinting with the AmpFISTR kit (Applied Biosystems; Foster City, CA). Primary cells were obtained from patients undergoing bone marrow aspiration after they had provided informed consent in compliance with the Declaration of Helsinki according to an Institutional Review

Board-approved protocol. CD20⁺ primary cells were purified by positive selection using magnetic-activated cell sorting with CD20⁺ microbeads (Miltenyi Biotec; Auburn, CA).

Cellular viability assays. Proliferation and viability assays were performed using the WST-1 reagent as previously described (18, 19). Briefly, cells were plated in triplicate and exposed to the conditions noted in the text, and premixed WST-1 cell proliferation reagent (Clontech Laboratories; Mountain View, CA) was added and used according to the manufacturer's specifications. Conversion of WST-1 to the formazan dye was measured at 650 nm using a Victor 3V plate-reader (Perkin Elmer Life Science; Waltham, MA), and viability data were prepared using GraphPad Prism version 6 (La Jolla, CA) showing the mean \pm the standard deviation. Experiments were performed in duplicate on different days, and results from one representative dataset are presented in the text.

Apoptosis and cell cycle analysis. Induction of apoptosis in cells treated with fostamatinib was detected by staining with an antibody to Annexin V and with ToPro3 (both from Life Technologies). Fluorescence-activated cell sorting (FACS) was then performed using a Fortessa FACS machine (Applied Biosystems; Foster City, CA). Cell cycle analysis was similarly performed after staining with 1 μ M propidium iodide (Sigma-Aldrich).

Western blotting. Cells were harvested, washed, and lysed with 1X lysis buffer (Cell Signaling Technology; Denver, MA) containing 1X Protease and 1X Phosphatase inhibitor mixtures (Roche Diagnostics; Indianapolis, IN). Lysates were then sonicated and clarified by centrifugation, and protein concentrations were determined using the DC Assay Kit (Bio-Rad; Hercules, CA). A total of 50 μ g of protein boiled in denaturing buffer (3% dithiothreitol, 0.1M Tris-HCl, pH 6.8, 4% sodium dodecylsulfate, 0.2% bromophenol blue, 20% glycerol) was separated

by gel electrophoresis, and transferred onto nitrocellulose membranes. These were blocked with Tris-buffered saline + 0.01% Tween 20 containing 5% non-fat milk, and then exposed to primary and secondary antibodies. Protein abundance was visualized using the Enhanced Chemiluminescence Kit according to the manufacturer's specification (Pierce Scientific; Rockford, IL) with autoradiography film (Eastman Kodak; Rochester, NY). The images were scanned and densitometry of the protein bands was performed using Image J Software (National Institute for Health) with normalization to β -actin as a loading control. Primary antibodies used included those against phospho-Tyr525/526 Syk (#12081), phospho-Tyr323 Syk (#2715), and total Syk (#2712), phospho-Tyr323 BTK (#2715) and total BTK (#3533), phospho-Ser117/Ser221 MAPK kinase (MEK; #9154) and total-MEK (#9122), phospho-Thr202/Tyr204 p44/42 MAPK (#4370) and total p44/42 MAPK (#9102), and phospho-Ser473 Akt (#4058) and total AKT (#9272), all of which were from Cell Signaling Technology (Danvers, MA). Loading controls were provided using an anti- β -Actin antibody (A1978) from Sigma-Aldrich.

Xenograft model. Experiments were performed in accordance with procedures and protocols approved by the MD Anderson Cancer Center Animal Care and Use Committee. Six-week old non-obese diabetic mice with severe combined immunodeficiency (NOD.Cg-*Prkdc*^{scid} *Il2rg*^{tm1Wjl}/SzJ) from Jackson Laboratories (Bar Harbor, ME) were injected subcutaneously with 1×10^7 MWCL-1 cells with Matrigel (BD Biosciences; San Jose, CA). Seven days after tumor formation, they were injected intraperitoneally with either phosphate-buffered saline, or this vehicle with fostamatinib to a final concentration of 80 mg/kg thrice weekly. The rate of growth was determined by measuring the tumor size twice weekly for a total of 45 days with calipers using the formula for an ellipsoid sphere: $(L \times W^2)/2 = \text{mm}^3$.

Statistical methods. The t-test or ANOVA, or their corresponding nonparametric methods (Wilcoxon rank-sum test or Kruskal-Wallis test), were used to detect differences for continuous variables between groups (20). Generalized linear regression models (21) were used to study the tumor growth over time in the xenograft model. Autoregressive (20) covariance structure was used to account for inter-mouse variability and the longitudinal nature of the data. An interaction between treatment and time is assessed to test the heterogeneity of slopes, i.e., the tumor growth rate. A two-sample t-test was used to compare the differences of tumor volume between the two groups at each time point. The transformation of logarithm to the base 2 of the tumor volume was used in the analyses to satisfy the normality assumption of the models, and Bonferroni multiplicity adjustment was applied for multiple comparisons. SAS version 9.2 (SAS; Cary, NC), R 2.80 and S-Plus version 8.04 (TIBCO Software, Inc.; Palo Alto, CA) were used to carry out the computations for all analyses.

Results

Fostamatinib induces apoptosis of Waldenström-derived cell lines. To determine if Syk inhibition could be valuable as an approach against Waldenström's, we examined the activity of fostamatinib against Waldenström-derived cell lines. Using an assay that measures the metabolism of WST-1 by mitochondrial succinate-tetrazolium reductase, we found that BCWM.1 cells exposed to fostamatinib showed a time- and concentration-dependent decrease in viability (Figure 1A). This was especially notable at 1 μ M of fostamatinib, which reduced viability by up to 45% after three days. In order to confirm these findings, we studied MWCL-1 cells, which were also sensitive to fostamatinib at 1 μ M, with a 53-60% reduction in viability after one to three days of exposure (Figure 1B), though 0.25 μ M showed activity as well after three days. Notably, these concentrations are well within those achieved by patients in phase I and pharmacokinetics studies of fostamatinib (22), where peak concentrations as high as 6 μ M were observed, suggesting that they are physiologically relevant.

Cell cycle analysis of BCWM.1 cells exposed to fostamatinib compared to vehicle controls revealed an increase in cells at G0/G1 from 67% to 76% (Figure 2A, left panel), and fewer cells were seen in S phase (27% to 21%). Similarly, MWCL-1 cells treated with fostamatinib tended to accumulate at G0/G1 (63% to 77%)(Figure 2A, right panel), with a reduction in the fraction in S phase (37% to 16%). In both models, fostamatinib increased the proportion of cells with a sub-G1 DNA content, which rose from 12% to 22% in BCWM.1 cells, and from 8% to 13% in MWCL-1 cells, suggesting the activation of programmed cell death. To examine for the latter, cells were stained with an antibody to Annexin V and with the nuclear dye ToPro3, and analyzed by cell sorting. Compared to vehicle-treated BCWM.1 cells (Figure 2B, upper panels), fostamatinib increased the proportion that were Annexin V+ from 4.6% to 26.9%, while in MWCL-1 cells this increased from 7.9% to 31.6% (Figure 2B, lower panels). At higher drug

concentrations, fostamatinib induced increased levels of apoptosis. Fostamatinib concentrations of 0.1, 1, 5, and 10 μ M induced staining with Annexin V in 18.5%, 24.1%, 28.2%, and 34.8% of BCWM.1 cells, respectively (Supplementary Figure 1A), and in 17.5%, 21.4%, 30.4%, and 57.0% of MWCL-1 cells, respectively (Supplementary Figure 1B). These findings indicate that Syk inhibition reduced viability in Waldenström-derived cell lines through a combination of cell cycle accumulation at G0/G1 and activation of apoptosis.

Activation of Syk is reduced by fostamatinib. In order to determine the impact of fostamatinib on Syk, we used Western blotting with antibodies specific for phospho-Tyr525/526, which are residues in the activation loop of the Syk kinase domain (23). In BCWM.1 cells (Figure 3A, left panel), fostamatinib reduced Syk activation in a concentration-dependent manner, with a 41% decrease in phospho-Syk after 1 μ M of this drug. A similar effect was seen in MWCL-1 cells, where fostamatinib reduced levels of phospho-Tyr525/526-Syk by up to 51% (Figure 3A, right panel). Also, we examined the impact on phosphorylation of Syk at Tyr323, which provides a binding site for the Cbl ubiquitin ligase (24, 25), and is therefore thought to be inhibitory of Syk activity. Interestingly, fostamatinib also reduced levels of phospho-Tyr323-Syk in BCWM.1 cells (Figure 3B, left panel) by up to 98% or more, and in MWCL-1 cells (Figure 3B, right panel) by up to 75%. Finally, to determine the net effect on Syk activity of fostamatinib in these models, we examined the levels of phospho-Tyr223-BTK, a modification that occurs as a result of auto-phosphorylation after trans-phosphorylation at Tyr551 in the BTK activation loop (26) (27). Whereas both BCWM.1 (Figure 3C, left panel) and MWCL-1 cells (Figure 3C, right panel), had substantial phospho-Tyr223-BTK levels at baseline, fostamatinib reduced these dramatically by up to 95% and 59%, respectively. These findings indicate that fostamatinib did reduce Syk activity and the activation status of the downstream intermediate BTK, which is itself a key contributor to the pathobiology of Waldenström's.

Fostamatinib inhibits downstream signaling cascades. Given the role of BCR signaling in activating key downstream signal transduction cascades, we next looked at its impact on p44/42 MAPK. Vehicle-treated BCWM.1 (Figure 4A, left panel) and MWCL-1 cells (Figure 4A, right panel) had abundant levels of phospho-Ser117/Ser221 MEK. After exposure to fostamatinib, however, a dose-dependent decrease was seen, with a reduction in phospho-MEK levels by up to 96% or more in both model systems. This led to inhibition of signaling through p44/42 MAPK, where phosphorylation at Thr202/Tyr204 was reduced by up to 97% and 74% in BCWM.1 (Figure 4B, left panel) and MWCL-1 cells (Figure 4B, right panel), respectively. Lastly, we looked at the impact of fostamatinib on Akt, a pathway whose activity has been described to influence homing and survival of Waldenström's cells (28). Consistent with a role for BCR signaling in activating Akt, Syk inhibition with fostamatinib dramatically reduced phospho-Ser473 Akt levels by up to 95-98% in BCWM.1 (Figure 4C, left panel) and MWCL-1 cells (Figure 4C, right panel).

Anti-tumor activity of fostamatinib. Since fostamatinib is clinically relevant in that it has been studied in patients with non-Hodgkin lymphomas (13), and is being evaluated in rheumatologic conditions (29), we next determined if it could show anti-tumor activity. We developed an *in vivo* xenograft based on MWCL-1 cells in immunodeficient mice which grew steadily in the vehicle-treated cohort (Figure 5A). In the fostamatinib-treated group, however, tumor growth was slower, and the difference between the two groups was different at a significance level of 0.0028 with adjustment of multiple comparisons (0.05/18 comparisons (1 comparison at each of 18 time points)). For example, the mean tumor volume of the control group on day 35 was larger than the one of the treatment group at a significance level of 0.0028 (p value = 0.0002). Also, we examined CD20⁺ cells isolated from bone marrow aspirates of patients with Waldenström's, and

found that fostamatinib was able to reduce viability in all of them (Figure 5B), and this was associated with a decrease in p44/42 MAPK activation (Figure 5C) in the one sample where sufficient cells were available to evaluate this by Western blotting.

Combination regimens enhance anti-Waldenström effects. Treatment of patients with Waldenström's in either the front-line or relapsed and/or refractory setting often involves the use of multi-drug regimens including corticosteroids, proteasome inhibitors, monoclonal antibodies, and alkylating agents (3, 30). To therefore see if fostamatinib could be considered not just as a stand-alone therapy, but also as part of other regimens, combination studies were performed. Dexamethasone as a single agent showed modest to no significant activity against either BCWM.1 or MWCL-1 cells (Figure 6A, left and right panels, respectively). Fostamatinib alone impacted upon viability in both cell lines, with an up to 28% reduction in MWCL-1 cells, for example. When the two were combined, however, enhanced activity was seen, especially in MWCL-1 cells, where an up to 80% decrease in viability was noted ($p < 0.01$). Proteasome inhibition with bortezomib showed activity and reduced viability by 36%, while fostamatinib with bortezomib reduced this further to 72% of controls in MWCL-1 cells ($p < 0.01$). Rituximab alone reduced viability by 25%, while an 84% reduction was seen with fostamatinib in combination with rituximab in MWCL-1 cells ($p < 0.01$). Lastly, bendamustine was examined, and also reduced viability in both cell lines (Supplementary Figure 2), with a reduction to 33% in MWCL-1 cells, which was enhanced further to 18% in combination with fostamatinib ($p < 0.01$).

It was also of interest in the context of combination therapy to determine if different sequences of addition of some of these agents could provide enhanced activity. To examine this possibility, BCWM.1 and MWCL-1 cells were exposed either first to fostamatinib for 24 hours and then to fostamatinib with dexamethasone or bortezomib for another 48 hours, or to dexamethasone or

bortezomib for 24 hours, followed by dexamethasone or bortezomib with fostamatinib for 48 hours. In BCWM.1 cells, there was an indication that addition of fostamatinib first led to a greater efficacy for the combination than if dexamethasone (Supplementary Figure 3A) or bortezomib (Supplementary Figure 3B) was added first. For example, in the case of the dexamethasone combination, adding fostamatinib first reduced viability to 22% of controls, while use of dexamethasone first reduced viability only to 30% of controls ($p < 0.01$). However, these two sequences were equally effective in reducing the viability in MWCL-1 cells with fostamatinib and either dexamethasone or bortezomib. Together, these data support the possibility that enhanced activity could be seen by combining fostamatinib with some of the agents currently used in the clinic against this disease.

Discussion

Recent studies of Waldenström macroglobulinemia have led to a greater understanding of the pathobiology of this disease, such as by identification of the L265P MYD88 mutation in 90% or more of patients (4-8). Whole genome sequencing has revealed that at least 10% of patients have somatic mutations in CXCR4 and AT rich interactive domain 1A (SWI-like)(ARID1A), while genes such as PR domain containing 2, with ZNF domain (PRDM2) and B-cell translocation gene 1, anti-proliferative (BTG1), among others, show frequent copy number abnormalities (31). A number of pathways have also been shown to play important roles in disease pathobiology, including, prominently, signaling through phosphoinositide 3-kinase/Akt/mammalian target of rapamycin (mTOR)(28, 32). This has led to the introduction of a variety of novel agents to therapy, including inhibitors of nuclear factor kappa B (33-35), of histone deacetylases (36), and of mTOR (37), among others. Perhaps because of these novel approaches, outcomes of patients with Waldenström macroglobulinemia in at least some studies have been improving (38). However, other analyses have suggested only a modest improvement (39), and though this may be due in part to different levels of access to novel drugs, since a minority of patients achieve complete remission, newer therapies are needed in either case.

In the current study, we evaluated the potential utility of the Syk inhibitor fostamatinib in pre-clinical models of Waldenström's. The rationale to consider that this could be of interest was based on the role of a number of BCR signaling-associated factors in disease pathobiology (4, 9), and earlier studies implicating Syk itself (10, 14). Consistent with this possibility, the Syk inhibitor fostamatinib at clinically relevant concentrations reduced the viability of Waldenström-derived cell lines (Figure 1) by inducing cell cycle arrest and apoptosis (Figure 2). This was associated with decreased activation of Syk and downstream BTK (Figure 3), as well as of signaling through p44/42 MAPK and Akt (Figure 4). Finally, fostamatinib as a single agent was

active against both a novel *in vivo* model of Waldenström and against primary cells (Figure 5), and showed enhanced activity in combination with clinically relevant agents, including dexamethasone, bortezomib, and rituximab (Figure 6).

Fostamatinib is the pro-drug of R406, and is an oral ATP-competitive inhibitor which showed activity in several pre-clinical models, including both *in vitro* and *in vivo* against diffuse large B-cell lymphoma (40). Friedberg et al. performed a phase I/II study of fostamatinib, which identified a dose of 200 mg twice daily for phase II testing (13), with dose-limiting toxicities of neutropenia, diarrhea, and thrombocytopenia. Interestingly, while the overall response rate (ORR) in relapsed diffuse large B-cell lymphoma was only 24% (4/17), in patients with more indolent disorders, such as chronic lymphocytic leukemia/small lymphocytic lymphoma, the ORR was 55% (6/11), with a median progression-free survival of 6.4 months. These data, along with our current studies, provide a rationale to consider translating fostamatinib to the clinic for patients with Waldenström either alone, or in combination with other standard agents.

Acknowledgements

This study was supported in part by The MD Anderson Cancer Center SPORE in Multiple Myeloma (P50 CA142509). The authors would like to thank the MD Anderson Flow Cytometry and Cellular Imaging Core Facility, and the Characterized Cell Line Core Facility, all of which are supported by the Cancer Center Support Grant (CA16672). R.Z.O. would also like to acknowledge support from the Florence Maude Thomas Cancer Research Professorship.

Abbreviations

ARID1A, AT rich interactive domain 1A (SWI-like); BCR, B-cell receptor; BTG1, B-cell translocation gene 1, anti-proliferative; BTK, Bruton's tyrosine kinase; CXCR4, C-X-C chemokine receptor type 4; FosD, fostamatinib disodium; IgM, immunoglobulin M; ITAMs, immunoreceptor tyrosine-based activation motifs; MAPK, mitogen activated protein kinase; MEK, MAPK kinase; mTOR, mammalian target of rapamycin; MYD88, Myeloid differentiation primary response gene 88; ORR, overall response rate; PBS, phosphate-buffered saline; PRDM2, PR domain containing 2, with ZNF domain; SFKs, Src family of kinases; Syk, Spleen tyrosine kinase; WM, Waldenström's macroglobulinemia

References

1. Efremov DG, Laurenti L. The Syk kinase as a therapeutic target in leukemia and lymphoma. *Expert Opin Investig Drugs*. 2011;20:623-36.
2. Rickert RC. New insights into pre-BCR and BCR signalling with relevance to B cell malignancies. *Nat Rev Immunol*. 2013;13:578-91.
3. Sahin I, Lelebjian H, Treon SP, Ghobrial IM. Waldenstrom macroglobulinemia: from biology to treatment. *Expert review of hematology*. 2014;7:157-68.
4. Treon SP, Xu L, Yang G, Zhou Y, Liu X, Cao Y, et al. MYD88 L265P somatic mutation in Waldenstrom's macroglobulinemia. *N Engl J Med*. 2012;367:826-33.
5. Gachard N, Parrens M, Soubeyran I, Petit B, Marfak A, Rizzo D, et al. IGHV gene features and MYD88 L265P mutation separate the three marginal zone lymphoma entities and Waldenstrom macroglobulinemia/lymphoplasmacytic lymphomas. *Leukemia*. 2013;27:183-9.
6. Xu L, Hunter ZR, Yang G, Zhou Y, Cao Y, Liu X, et al. MYD88 L265P in Waldenstrom macroglobulinemia, immunoglobulin M monoclonal gammopathy, and other B-cell lymphoproliferative disorders using conventional and quantitative allele-specific polymerase chain reaction. *Blood*. 2013;121:2051-8.
7. Varettoni M, Arcaini L, Zibellini S, Boveri E, Rattotti S, Riboni R, et al. Prevalence and clinical significance of the MYD88 (L265P) somatic mutation in Waldenstrom's macroglobulinemia and related lymphoid neoplasms. *Blood*. 2013;121:2522-8.
8. Jimenez C, Sebastian E, Chillon MC, Giraldo P, Mariano Hernandez J, Escalante F, et al. MYD88 L265P is a marker highly characteristic of, but not restricted to, Waldenstrom's macroglobulinemia. *Leukemia*. 2013;27:1722-8.
9. Yang G, Zhou Y, Liu X, Xu L, Cao Y, Manning RJ, et al. A mutation in MYD88 (L265P) supports the survival of lymphoplasmacytic cells by activation of Bruton tyrosine kinase in Waldenstrom macroglobulinemia. *Blood*. 2013;122:1222-32.

10. Ciric B, VanKeulen V, Rodriguez M, Kyle RA, Gertz MA, Pease LR. Clonal evolution in Waldenstrom macroglobulinemia highlights functional role of B-cell receptor. *Blood*. 2001;97:321-3.
11. Aalipour A, Advani RH. Bruton tyrosine kinase inhibitors: a promising novel targeted treatment for B cell lymphomas. *British journal of haematology*. 2013;163:436-43.
12. Treon SP, Tripsas CK, Yang G, Cao Y, Xu L, Hunter Z, et al. A prospective multicenter study of the Bruton's tyrosine kinase inhibitor ibrutinib in patients with relapsed or refractory Waldenstrom's macroglobulinemia. *Blood*. 2013;122:Abstract 251.
13. Friedberg JW, Sharman J, Sweetenham J, Johnston PB, Vose JM, Lacasce A, et al. Inhibition of Syk with fostamatinib disodium has significant clinical activity in non-Hodgkin lymphoma and chronic lymphocytic leukemia. *Blood*. 2010;115:2578-85.
14. Gertz MA. Waldenstrom macroglobulinemia: 2011 update on diagnosis, risk stratification, and management. *Am J Hematol*. 2011;86:411-6.
15. Ditzel Santos D, Ho AW, Tournilhac O, Hatjiharissi E, Leleu X, Xu L, et al. Establishment of BCWM.1 cell line for Waldenstrom's macroglobulinemia with productive in vivo engraftment in SCID-hu mice. *Exp Hematol*. 2007;35:1366-75.
16. Cao Y, Hunter ZR, Liu X, Xu L, Yang G, Chen J, et al. The WHIM-like CXCR4 somatic mutation activates AKT and ERK, and promotes resistance to ibrutinib and other agents used in the treatment of Waldenstrom's Macroglobulinemia. *Leukemia*. 2014.
17. Hodge LS, Novak AJ, Grote DM, Braggio E, Ketterling RP, Manske MK, et al. Establishment and characterization of a novel Waldenstrom macroglobulinemia cell line, MWCL-1. *Blood*. 2011;117:e190-7.
18. Bjorklund CC, Ma W, Wang ZQ, Davis RE, Kuhn DJ, Kornblau SM, et al. Evidence of a role for activation of Wnt/beta-catenin signaling in the resistance of plasma cells to lenalidomide. *J Biol Chem*. 2011;286:11009-20.

19. Jones RJ, Baladandayuthapani V, Neelapu S, Fayad LE, Romaguera JE, Wang M, et al. HDM-2 inhibition suppresses expression of ribonucleotide reductase subunit M2, and synergistically enhances gemcitabine-induced cytotoxicity in mantle cell lymphoma. *Blood*. 2011;118:4140-9.
20. Woolson RF, Clarke WR. *Statistical methods for the analysis of biomedical data*. 2nd ed. New York: Wiley-Interscience; 2002.
21. Zeger SL, Liang KY. Longitudinal data analysis for discrete and continuous outcomes. *Biometrics*. 1986;42:121-30.
22. Baluom M, Grossbard EB, Mant T, Lau DT. Pharmacokinetics of fostamatinib, a spleen tyrosine kinase (SYK) inhibitor, in healthy human subjects following single and multiple oral dosing in three phase I studies. *Br J Clin Pharmacol*. 2013;76:78-88.
23. Zhang J, Billingsley ML, Kincaid RL, Siraganian RP. Phosphorylation of Syk activation loop tyrosines is essential for Syk function. An in vivo study using a specific anti-Syk activation loop phosphotyrosine antibody. *J Biol Chem*. 2000;275:35442-7.
24. Deckert M, Elly C, Altman A, Liu YC. Coordinated regulation of the tyrosine phosphorylation of Cbl by Fyn and Syk tyrosine kinases. *J Biol Chem*. 1998;273:8867-74.
25. Rao N, Ghosh AK, Ota S, Zhou P, Reddi AL, Hakezi K, et al. The non-receptor tyrosine kinase Syk is a target of Cbl-mediated ubiquitylation upon B-cell receptor stimulation. *EMBO J*. 2001;20:7085-95.
26. Rawlings DJ, Scharenberg AM, Park H, Wahl MI, Lin S, Kato RM, et al. Activation of BTK by a phosphorylation mechanism initiated by SRC family kinases. *Science*. 1996;271:822-5.
27. Park H, Wahl MI, Afar DE, Turck CW, Rawlings DJ, Tam C, et al. Regulation of Btk function by a major autophosphorylation site within the SH3 domain. *Immunity*. 1996;4:515-25.
28. Leleu X, Jia X, Runnels J, Ngo HT, Moreau AS, Farag M, et al. The Akt pathway regulates survival and homing in Waldenstrom macroglobulinemia. *Blood*. 2007;110:4417-26.

29. Simmons DL. Targeting kinases: a new approach to treating inflammatory rheumatic diseases. *Curr Opin Pharmacol.* 2013;13:426-34.
30. Ansell SM, Kyle RA, Reeder CB, Fonseca R, Mikhael JR, Morice WG, et al. Diagnosis and management of Waldenstrom macroglobulinemia: Mayo stratification of macroglobulinemia and risk-adapted therapy (mSMART) guidelines. *Mayo Clin Proc.* 2010;85:824-33.
31. Hunter ZR, Xu L, Yang G, Zhou Y, Liu X, Cao Y, et al. The genomic landscape of Waldenstrom macroglobulinemia is characterized by highly recurring MYD88 and WHIM-like CXCR4 mutations, and small somatic deletions associated with B-cell lymphomagenesis. *Blood.* 2014;123:1637-46.
32. Roccaro AM, Sacco A, Husu EN, Pitsillides C, Vesole S, Azab AK, et al. Dual targeting of the PI3K/Akt/mTOR pathway as an antitumor strategy in Waldenstrom macroglobulinemia. *Blood.* 2010;115:559-69.
33. Leleu X, Eeckhoute J, Jia X, Roccaro AM, Moreau AS, Farag M, et al. Targeting NF-kappaB in Waldenstrom macroglobulinemia. *Blood.* 2008;111:5068-77.
34. Chen CI, Kouroukis CT, White D, Voralia M, Stadtmauer E, Stewart AK, et al. Bortezomib is active in patients with untreated or relapsed Waldenstrom's macroglobulinemia: a phase II study of the National Cancer Institute of Canada Clinical Trials Group. *Journal of clinical oncology : official journal of the American Society of Clinical Oncology.* 2007;25:1570-5.
35. Treon SP, Hunter ZR, Matous J, Joyce RM, Mannion B, Advani R, et al. Multicenter clinical trial of bortezomib in relapsed/refractory Waldenstrom's macroglobulinemia: results of WMCTG Trial 03-248. *Clinical cancer research : an official journal of the American Association for Cancer Research.* 2007;13:3320-5.
36. Ghobrial IM, Campigotto F, Murphy TJ, Boswell EN, Banwait R, Azab F, et al. Results of a phase 2 trial of the single-agent histone deacetylase inhibitor panobinostat in patients with relapsed/refractory Waldenstrom macroglobulinemia. *Blood.* 2013;121:1296-303.

37. Ghobrial IM, Gertz M, Laplant B, Camoriano J, Hayman S, Lacy M, et al. Phase II trial of the oral mammalian target of rapamycin inhibitor everolimus in relapsed or refractory Waldenstrom macroglobulinemia. *Journal of clinical oncology : official journal of the American Society of Clinical Oncology*. 2010;28:1408-14.
38. Kristinsson SY, Eloranta S, Dickman PW, Andersson TM, Turesson I, Landgren O, et al. Patterns of survival in lymphoplasmacytic lymphoma/Waldenstrom macroglobulinemia: a population-based study of 1,555 patients diagnosed in Sweden from 1980 to 2005. *Am J Hematol*. 2013;88:60-5.
39. Kastiris E, Kyrtonis MC, Hatjiharissi E, Symeonidis A, Michalis E, Repoussis P, et al. No significant improvement in the outcome of patients with Waldenstrom's macroglobulinemia treated over the last 25 years. *Am J Hematol*. 2011;86:479-83.
40. Witzig TE, Gupta M. Signal transduction inhibitor therapy for lymphoma. *Hematology Am Soc Hematol Educ Program*. 2010;2010:265-70.

Figure Legends

Figure 1. Fostamatinib reduces viability in Waldenstrom macroglobulinemia cells.

BCWM.1 (A) and MWCL-1 cells (B) were seeded in 96 wells plates at 10,000 cells per well and treated with vehicle, 0.25, or 1 μ M concentrations of fostamatinib for 24, 48, or 72 hours, as indicated. Cell viability was assayed using the tetrazolium reagent WST-1, and data shown are representative of one of two independent experiments, each performed in triplicate, and are presented as mean \pm S.D. A "***" indicates a statistical significance at a level of $p < 0.01$ compared to vehicle-treated controls using the student's t-test.

Figure 2. Fostamatinib induces cell cycle arrest and apoptosis.

BCWM.1 and MWCL-1 cells treated with either vehicle or 1 μ M of fostamatinib for 24 hours were examined for their cell cycle profile (A) by propidium iodine staining followed by analysis with flow cytometry of 10,000 events. Apoptosis was assessed after these same conditions (B) by staining cells with an antibody to Annexin V and the nuclear stain ToPro3. The "No Dye" panels contain cells that have been exposed to Annexin V staining buffer but not to either Annexin V or ToPro3.

Figure 3. Fostamatinib inhibits activation of Syk and BTK.

BCWM.1 and MWCL-1 cells treated with either vehicle or fostamatinib at the indicated concentrations for two hours were harvested and lysed, and protein extracts were analyzed by Western blotting. The activation status of Syk (A, B) and BTK (C) was probed with phospho-specific antibodies using β -Actin as well as the levels of total, non-phosphorylated Syk and BTK as controls. Data shown are representative of one of three independent experiments.

Figure 4. Fostamatinib inhibits activation of the MAPK and Akt pathways.

BCWM.1 and MWCL-1 cells treated as above were analyzed by Western blotting for the activation status of MEK, p44/42 MAPK, and Akt with phospho-specific antibodies as described earlier.

Figure 5. Fostamatinib shows activity against an *in vivo* model and primary cells.

Immunodeficient mice were injected subcutaneously with 1×10^6 MWCL-1 cells, and seven days after implantation they were randomized to receive vehicle or fostamatinib at 85 mg/kg daily **(A)**. Tumor growth was monitored by caliper measurements and plotted against time. Primary cells from four patients with Waldenström's purified using CD20 microbeads were then exposed to vehicle or 1 μ M of fostamatinib for 24 or 48 hours as indicated **(B)**. Cell viability was measured by using the tetrazolium reagent WST-1, and all data points were normalized to the vehicle controls, which were arbitrarily set at 100%. Whole protein cell lysates of cells from one patient were prepared **(C)** from the CD20+ fraction and treated with fostamatinib or vehicle control for two hours. Western blotting with phospho-specific and total-p44/42 MAPK antibodies was then performed.

Figure 6. Fostamatinib shows enhanced activity in combination with other agents.

BCWM.1 or MWCL-1 cells were treated for 48 hours with vehicle, dexamethasone alone at 5 μ M, fostamatinib at 1.6 μ M, or with the combination with dexamethasone **(A)**. Cell viability was determined with WST-1 as described above, and experiments were replicated five times on different days, with one representative set shown. "***" indicates $p < 0.01$ for the combination compared to the standard agent in each panel, while "##" indicates $p < 0.01$ compared to fostamatinib. BCWM.1 or MWCL-1 cells were also exposed to either single-agent bortezomib (5 nM)**(B)** or rituximab (0.1 mg/mL)**(C)**, and combinations with fostamatinib were examined as

described above. Statistical differences were at $p < 0.01$ for all the panels except for BCWM.1 cells treated with rituximab and fostamatinib, in which the p value was < 0.05 .

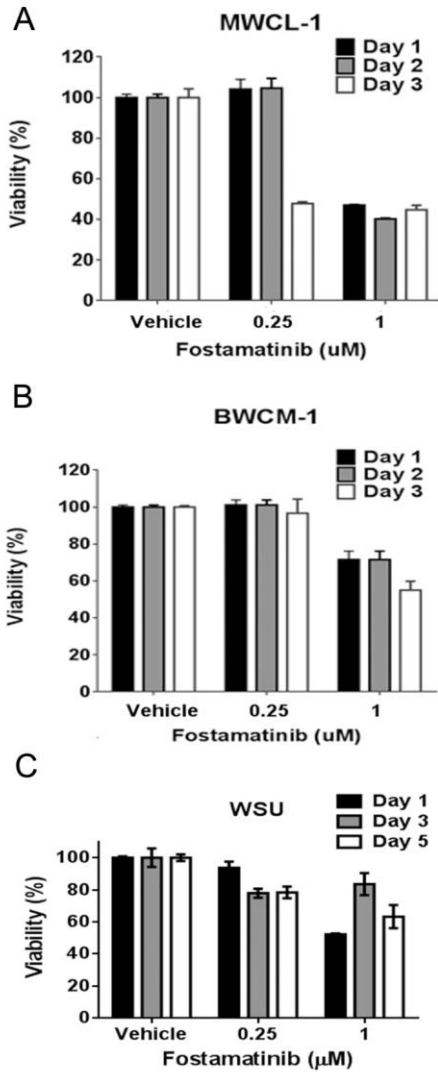


Figure 1

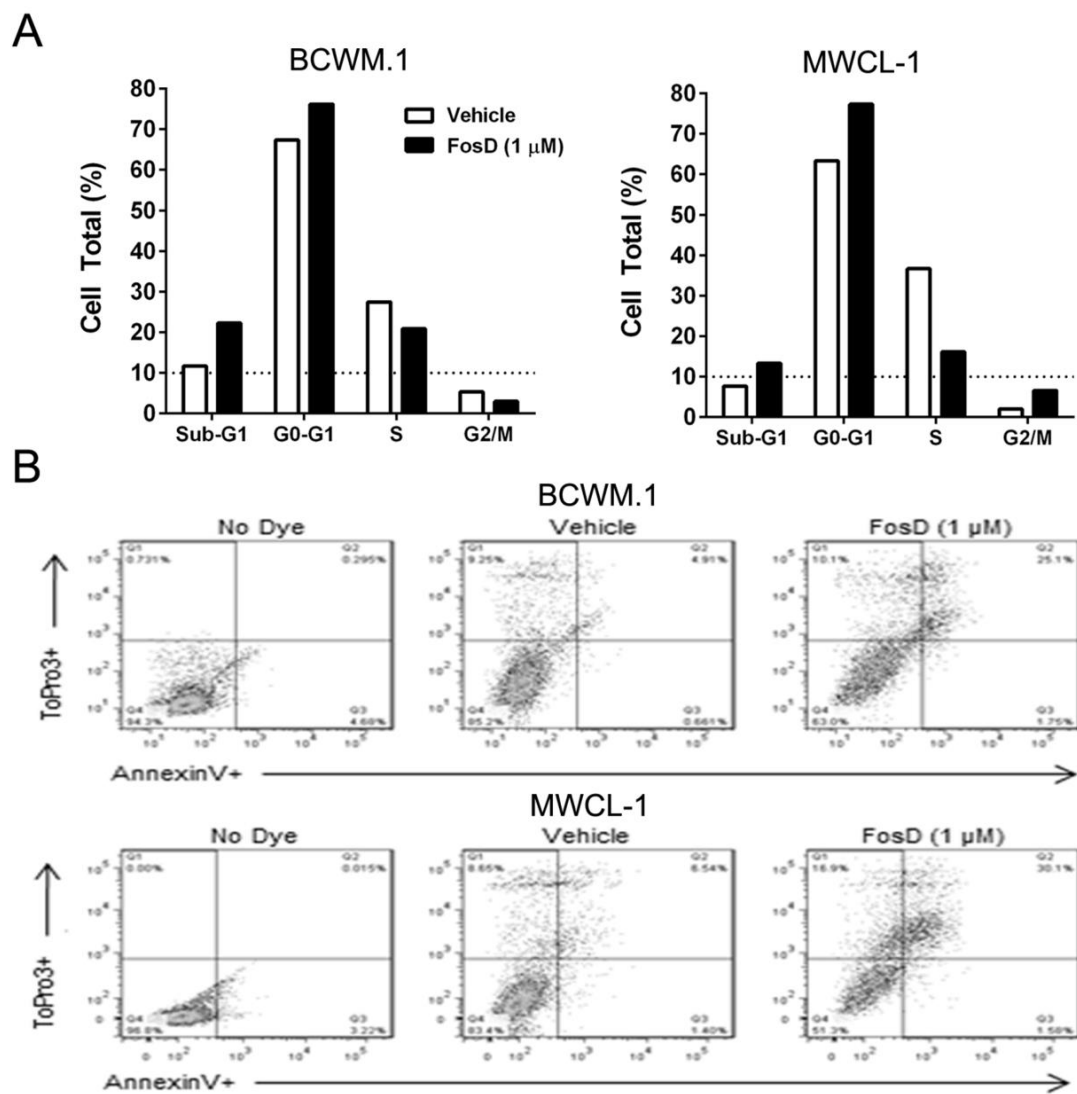


Figure 2

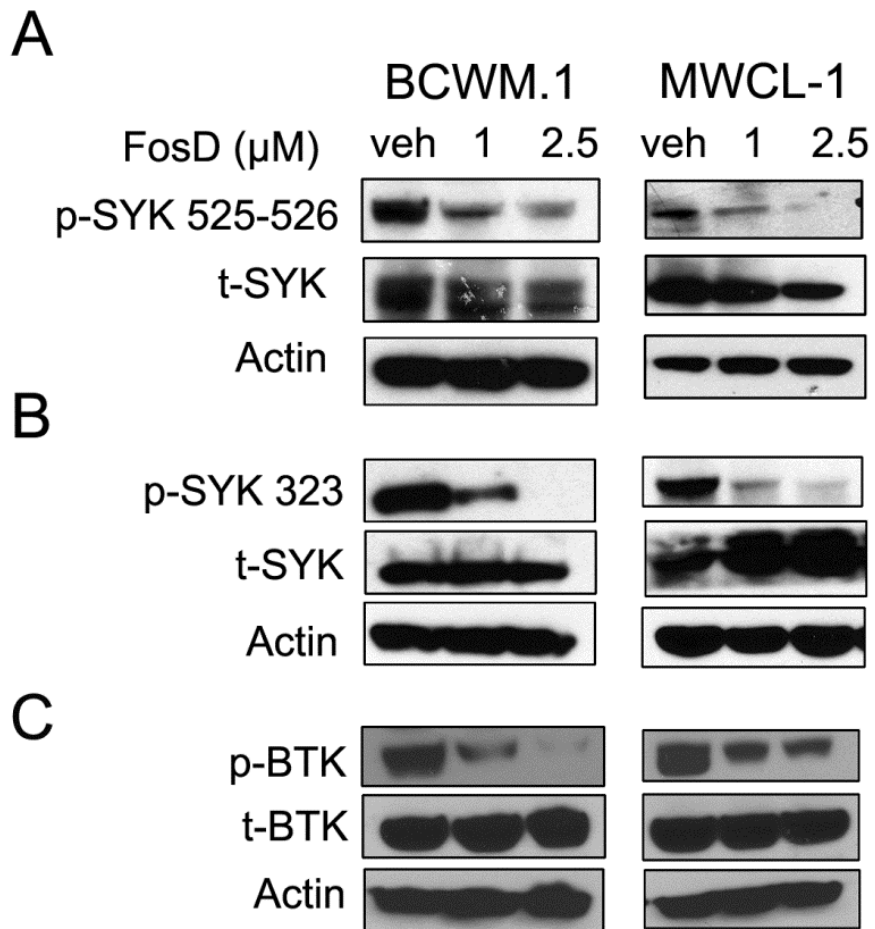


Figure 3

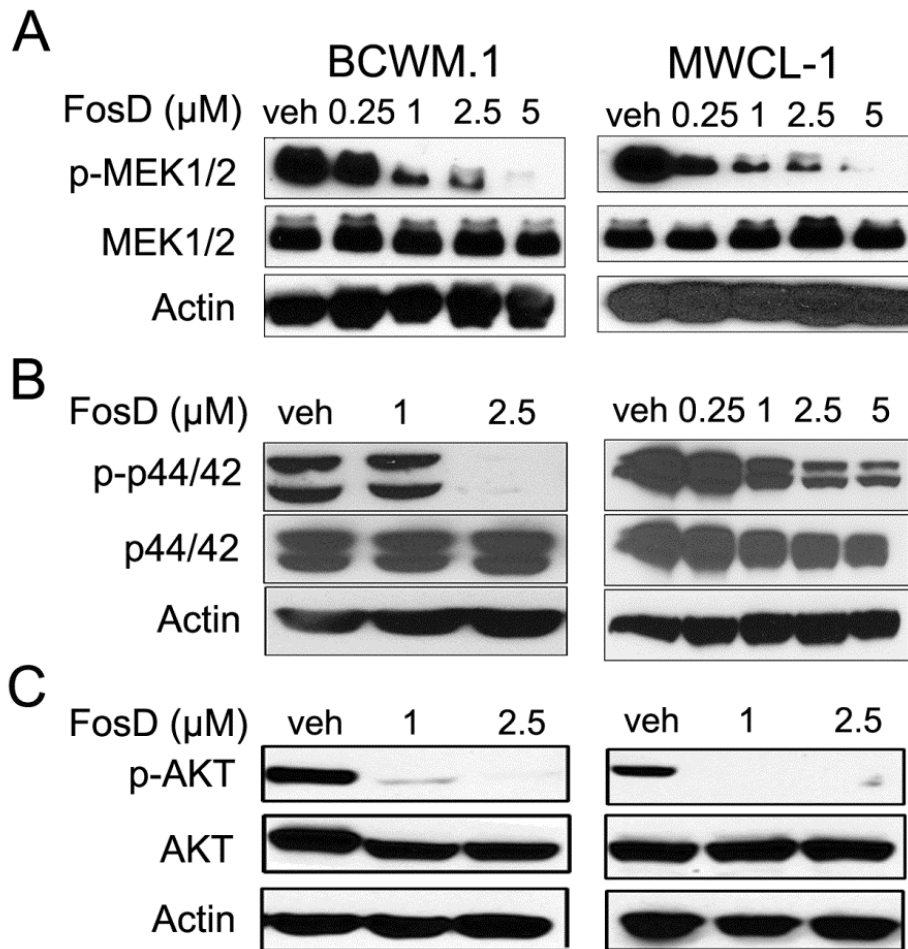


Figure 4

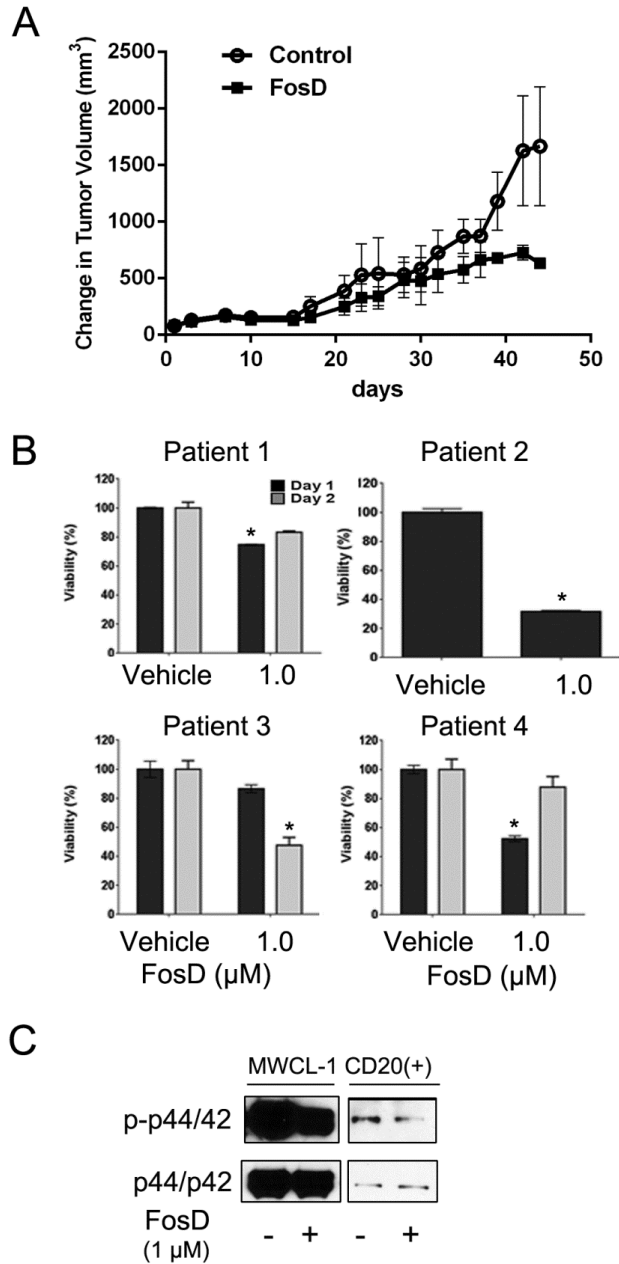


Figure 5

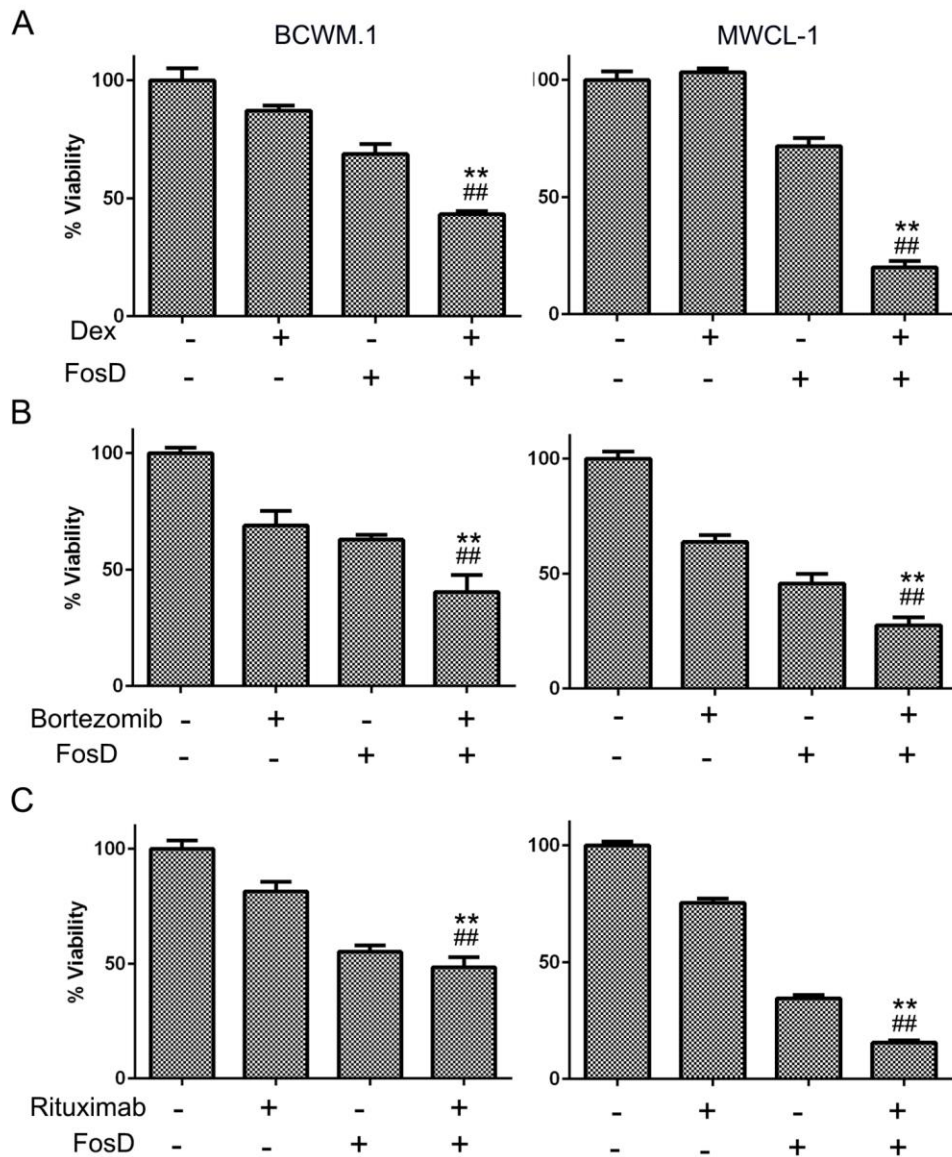
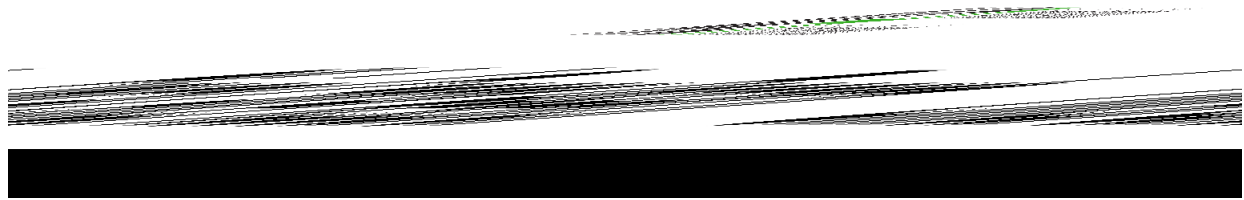


Figure 6



Targeting the Spleen Tyrosine Kinase with Fostamatinib as a Strategy Against Waldenström's Macroglobulinemia

Isera Kuiatse, Veerabhadran Baladandayuthapani, Heather Y Lin, et al.

Clin Cancer Res Published OnlineFirst March 6, 2015.

Updated version	Access the most recent version of this article at: doi: 10.1158/1078-0432.CCR-14-1462
Supplementary Material	Access the most recent supplemental material at: http://clincancerres.aacrjournals.org/content/suppl/2015/03/07/1078-0432.CCR-14-1462.DC1.html
Author Manuscript	Author manuscripts have been peer reviewed and accepted for publication but have not yet been edited.

E-mail alerts [Sign up to receive free email-alerts](#) related to this article or journal.

Reprints and Subscriptions To order reprints of this article or to subscribe to the journal, contact the AACR Publications Department at pubs@aacr.org.

Permissions To request permission to re-use all or part of this article, contact the AACR Publications Department at permissions@aacr.org.